

# New tilted-poles Wien filter with enhanced performance<sup>a)</sup>

E. Leal-Quiros and M. A. Prefas

Fusion Research Laboratory, Nuclear Engineering Program, University of Missouri-Columbia, Columbia, Missouri 65211

(Received 15 March 1988; accepted for publication 10 August 1988)

The Wien filter is an  $E \times B$  deflecting analyzer with the electrostatic field perpendicular to the magnetostatic field. The twofold functions of the Wien filter are as an energy analyzer as well as a mass analyzer. It has very high resolution for paraxial charged-particle beams with  $V = E/B$ , the Wien velocity. Two Wien filters, a tilted-poles Wien filter, and a classical parallel-rectangular-poles Wien filter were built and tested for electrons up to 3.5 keV and protons beams of 200 eV. (The tilted-poles Wien filter is a new diagnostic developed by the authors.) The performance of the two is compared, and the tilted-poles Wien filter has superior resolution to the classical Wien filter. Both Wien filters appear to have features useful for high-temperature plasma diagnostics, including simultaneous measurement of energy and mass spectra, and high resolution.

## INTRODUCTION

The  $E \times B$  analyzer has been used in a broad range of applications. One such use was for the measurement of the velocity and composition of the solar wind ( $\alpha, \beta, p^+, D^+$ ) by the Mariner 2 space probe.<sup>1</sup> Additionally,  $E \times B$  analyzers have found application in mass spectroscopy,<sup>2</sup> molecular spectroscopy,<sup>3</sup> electron microscopes,<sup>4</sup> and fusion experiments.<sup>5-7</sup> We report here a new diagnostic called the tilted-poles (TP) Wien filter and its potential as a high-temperature plasma diagnostic, which allows both mass and energy discrimination simultaneously.

The classical rectangular-parallel-poles Wien filter permits a straight-through path for charged-particle beams. For some applications, such as plasma diagnostics and scattering experiments, this feature is an advantage of the Wien filter over other analyzers such as magnetic selectors, which usually produce a curved trajectory of the beam particles (i.e., the analyzed particles emerge at angles of 60°, 90°, or 180° to the input). Among other things, the straight-through path allows the system to be optically aligned and the entire beam can be directed toward either the collision region or the detector.<sup>8</sup>

We will discuss two types of Wien filters (Fig. 1): the classical design using rectangular-parallel magnetic poles and a new design developed by the authors using tilted magnetic poles.<sup>8</sup> The filters are designed to work with protons or electrons. The solution to the equations of motion and the trajectories of the particles in both of the  $E \times B$  detector designs will be discussed. Additionally, the correction of the astigmatism problem inherent in the classical Wien filter through the use of tilted magnetic poles will be shown. Finally, a comparison of the behavior of the two  $E \times B$  analyzers will be made, through the examination of the spectrum for electrons and protons of different energy.

## I. THEORETICAL CONDITIONS FOR THE CLASSICAL WIEN FILTER

From the Lorentz equation,

$$ma = eE + eV \times B, \quad (1)$$

the motion of charged particles in crossed electric and magnetic fields is given by

$$\omega = \eta B, \quad (2)$$

$$R_0 = \eta E / \omega^2, \quad (3)$$

where  $\eta = e/m$ ,  $B = [B_x, 0, 0]$  and  $E = [0, E_y, 0]$  are constant and homogeneous.  $R_0$  and  $\omega$  are the cyclotron radius and the cyclotron frequency;  $e$ ,  $m$ , and  $\eta$  are the charge, mass, and specific charge; and  $a$  is acceleration.

The equations of motion for the classical Wien filter are

$$\frac{d^2x}{dt^2} = 0, \quad (4)$$

$$\frac{d^2y}{dt^2} = -\eta E - \eta B V_z, \quad (5)$$

$$\frac{d^2z}{dt^2} = \eta B V_y. \quad (6)$$

The solutions are

$$x = pt + Q, \quad (7)$$

$$y = R \sin(\omega t + \theta) - \eta E / \omega^2 - I / \omega, \quad (8)$$

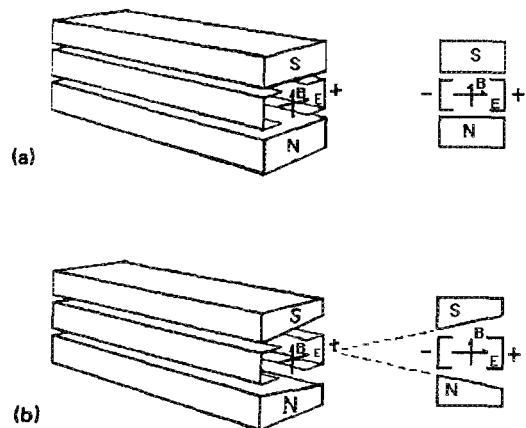


FIG. 1. Two kinds of Wien filters: (a) parallel rectangular poles and (b) tilted poles.

$$z = -R \cos(\omega t + \theta) - Et/B + K/\omega. \quad (9)$$

The constants  $p$ ,  $Q$ ,  $R$ ,  $\theta$ ,  $K$ , and  $I$  depend on the initial conditions, and several cases will be considered: For  $V_0 = (\dot{x}_0^2 + \dot{y}_0^2 + \dot{z}_0^2)^{1/2}$ , with  $E \neq 0$ ,  $B \neq 0$ , and  $t = 0$ , the solution becomes

$$x = x_0 + V_0 t, \quad (10)$$

$$y = R \sin(\omega t + \theta) - \eta E/\omega^2 - I/\omega, \quad (11)$$

$$z = -R \cos(\omega t + \theta) - Et/B + K/\omega. \quad (12)$$

The two main functions of the Wien filter, as a mass separator and as an energy filter, can be seen in Figs. 2 and 3.

If a small variation of the energy or direction  $\delta$  (incidence angle) is permitted, then there are two cases: (i) The energy focus is found at  $z = -\pi R_0$ , if  $\delta = 0$ , where  $\delta =$  incidence angle (Fig. 2). (ii) If  $\delta \neq 0$ , an error is introduced in the value of energy dispersion,  $dE_k/E_k$ , which is reduced by  $3\delta^2$  by the dispersion of the beam<sup>9</sup> in Fig. 4

$$\frac{d_v}{R_0} = \frac{dE_k}{E_k} - 3\delta^2.$$

As can be seen in the previous derivations, the Wien filter is an *energy selector*<sup>9</sup> with an angular focus of first order in the perpendicular plane to the  $Z$  axis.

## II. THE ASTIGMATISM PROBLEM

In the classical configuration of parallel-rectangular magnetic poles, the crossed field separator ( $E \times B$ ), for ions with  $V_0 = E_0/B_0$ , causes focusing of the emerging beam. The observed focus is not axisymmetric, and thus astigmatism is introduced into the beam.

Seliger<sup>10</sup> predicted theoretically that with suitable tilted magnetic poles, an  $E \times B$  separator can be used to focus the emerging beam in both the  $x$  and  $y$  directions. The configuration and the dynamic equation for this case are given in Fig.

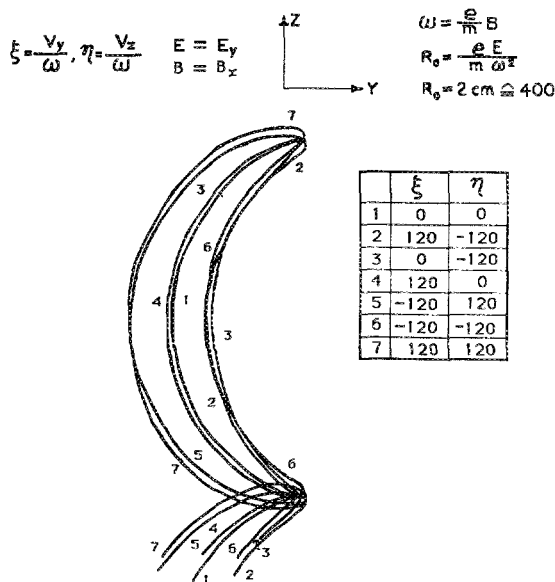


FIG. 2. Trajectory of electrons starting within the fields region. All particles are focused in  $Z = 2\pi R$  because they have equal mass (mass focus). The particles with same velocity are focused (velocity filter), and the different energies are separated at  $Z = \pi R$ .

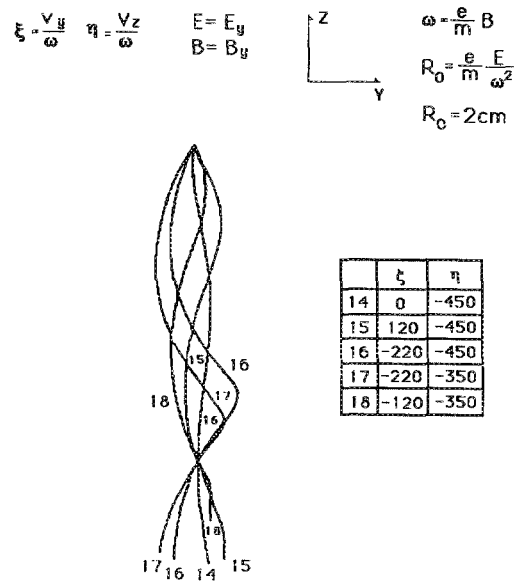


FIG. 3. The particles enter at the device with different velocities, but at  $Z = 2\pi R$  all particles with the same mass are focused.

5. However, there seems to be no experimental work on these tilted separators and their effect on focused beams.

Astigmatism occurs because the component of the beam velocity in the direction of the magnetic field is not affected by the field. An entering beam with a circular cross section emerges with an elliptical cross section<sup>8</sup> [Figs. 5(a) and 5(b)]. To eliminate the astigmatism, the fields must produce a transverse restoring force that is linear in the axial

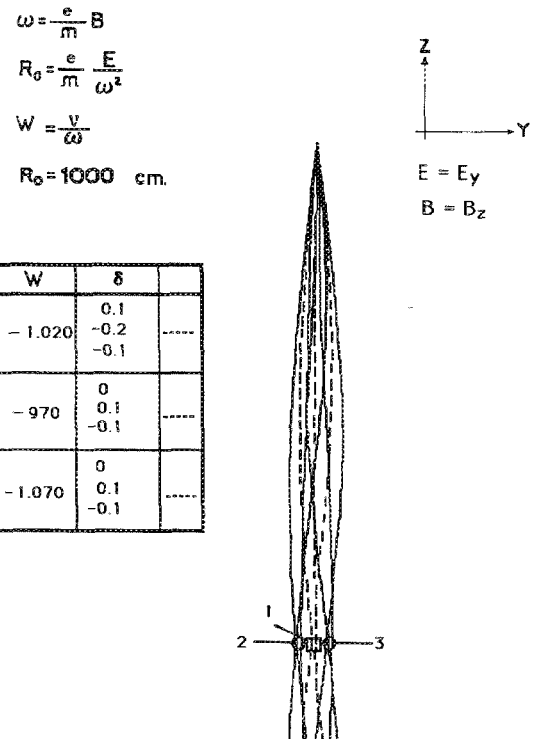


FIG. 4. A beam with three different energies is entering to the device. At  $Z = 2\pi R$  the particles with the same energy are focused and the three energies are separated. However there is dispersion in the energy focus because the incidence angle is different in each group with the same energy.

	Fields	Equations of Motion	Focusing x Direction y Direction	
a)	$E_x = 0$ $E_y = E_0$ $B_x = B_0$ $B_y = 0$	$\ddot{x} = 0$ $\ddot{y} = -\eta_0^2 B_0^2 y$ $\ddot{z} = \eta_0^2 B_0^2 y$ $\eta_0 = e/m$ $v_0 = (2\eta_0 V_0)^{1/2}$	NO YES	
b)	$E_x = 0$ $E_y = E_0$ $B_x = B_0(1 - y/R_0)$ $B_y = B_0 x/R_0$ $R_0 = 2V_0/E_0$	$\ddot{x} = -\eta_0^2 B_0^2 x$ $\ddot{y} = 0$ $\ddot{z} = \eta_0 \dot{y} B_0$	YES NO	
c)	$E_x = 0$ $E_y = E_0$ $B_x = B_0(1 - y/R_0)$ $B_y = -B_0 x/2R_0$	$\ddot{x} = -\eta_0^2 B_0^2 x/2$ $\ddot{y} = -\eta_0^2 B_0^2 y/2$ $\ddot{z} = \eta_0 \dot{y} B_0$	YES YES	

FIG. 5. Motion equations in the Seliger models. The kinds (a) and (c) were built.

direction. Astigmatism occurs when the restoring force is not axisymmetric. The astigmatism of the beam can be completely eliminated using the configuration of Fig. 5(c), where the force in  $x$  and  $y$  directions are the same.

### III. EQUATIONS OF MOTION FOR THE TILTED-POLES WIEN FILTER

For the tilted magnetic poles, using the Seliger<sup>10</sup> equations for electrons,

$$\ddot{x}_0 = -\frac{1}{2}[(e/m)B_0]^2 x, \quad (13)$$

$$\ddot{y}_0 = -\frac{1}{2}[(e/m)B_0]^2 y, \quad (14)$$

$$\ddot{z}_0 = (e/m)\dot{y}_0 B_0. \quad (15)$$

Suppositions: (a) There is no space charge present. (b)  $\dot{x}_0/V_0 \ll 1$  and  $\dot{y}_0/V_0 \ll 1$  (paraxial beams):

$$\eta = e/m_0,$$

$$V_0 = E_0/B_0,$$

(c)  $x/y_0 \ll 1$  and  $y/R_0 \ll 1$  (paraxial beams):

$$R_0 = \frac{v_0}{\eta_0 B_0} = \frac{2v_0}{E_0} = \frac{eE_0}{m\omega^2},$$

$$\omega = (e/m)B.$$

For the initial conditions,

$$(x_0, y_0, 0), [\dot{x}_0, \dot{y}_0, v_0(1 + y_0/R_0)],$$

the solutions are

$$\frac{x}{R_0} = \left(\frac{x_0}{R_0}\right)\cos\beta + \sqrt{2}\left(\frac{\dot{x}_0}{V_0}\right)\sin\beta, \quad (16)$$

$$\frac{y}{R_0} = \left(\frac{y_0}{R_0}\right)\cos\beta + \sqrt{2}\left(\frac{\dot{y}_0}{V_0}\right)\sin\beta, \quad (17)$$

$$\frac{z}{R_0} = \frac{\beta}{\sqrt{2}} = \frac{\eta_0 B_0 t}{\sqrt{2}}. \quad (18)$$

If we define  $z = L$ , then  $\beta = L/\sqrt{2}R_0$  and  $f = R_0\sqrt{2}/\sin\beta = \text{mass focus}$ , where  $L$  is the length of the filter and  $R_0$  is the cyclotron radius. The paths of the electrons in the tilted-poles Wien filter are shown in Figs. 6 and 7.

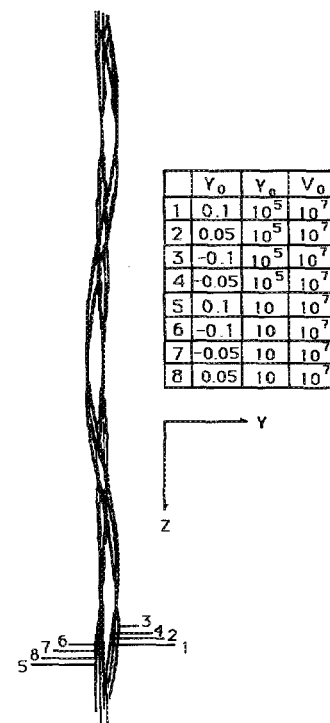


FIG. 6. Trajectory of the electrons in the tilted Wien filter. The initial beams have two different incidence angles.

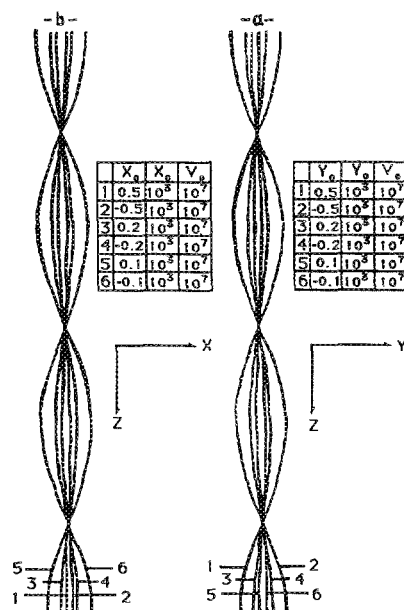


FIG. 7. Trajectory of the electrons in the tilted Wien filter where the astigmatism is completely eliminated.

#### IV. EXPERIMENT

Two types of Wien filters were built: a classical Wien filter with parallel-rectangular poles (Fig. 8) and a new configuration with suitable tilted poles (Fig. 1). The electromagnet was located inside the vacuum chamber where the magnetic field could be varied. The particles follow a cyclo-

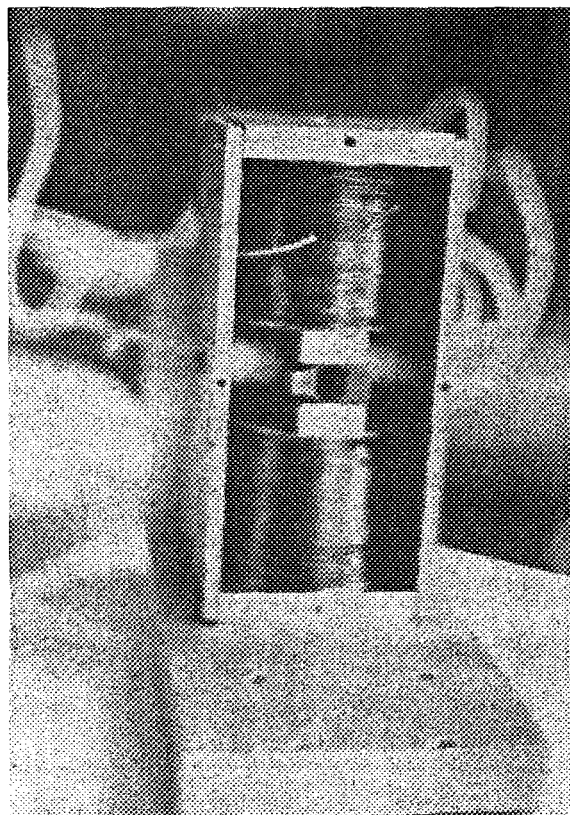


FIG. 8. Wien filter.

dal path and, for  $R_0 = 6/\pi$  cm, the gap between the magnet poles,  $d = 1$  cm and  $\phi_0 = E_0 R_0$ , have an energy focus (independent of  $m$ ) at  $z = \pi R_0$ , when  $\phi_d = (\pi/3)\phi_0 \approx \phi_0$ , and a mass focus at  $z = 2\pi R_0$ , when  $\phi_d = 2\phi_0$ . Here  $\phi_d$  is the deflecting potential between the capacitor plates and  $\phi_0$  is the acceleration potential.

If the initial velocity of the particles,  $V_0 = (2\eta_0\phi_0)^{1/2}$ , equals the Wien velocity,  $V_w = E_0/B_0$ , i.e.,

$$V_0 = E_0/B_0,$$

then

$$E_0 = \frac{V_0^2}{\eta R_0} = \frac{2\phi_0}{R_0} = \frac{\phi_d}{d},$$

and

$$B_0 = V_0/\eta R_0.$$

The magnetic field for obtaining an energy focus is

$$B_0 = 1.7 \times 10^{-4} \sqrt{\phi_0} \text{ T (for electrons),}$$

or

$$B_0 = 72.25 \times 10^{-4} \sqrt{\phi_0} \text{ T (for protons),}$$

while the magnetic field for obtaining a mass focus is twice that for an energy focus.

The optimal configuration found for the capacitor is shown in Fig. 9. This configuration was chosen because it has more homogeneity in the electric field, and the field vectors are perpendicular to the equipotential surfaces,  $E = -\nabla\phi$ .

The design of the magnet and its hysteresis are shown in Figs. 10 and 11, respectively. However, in Fig. 12, a "tiny hysteresis" shows that, in the case where electrons need to be selected, the magnetic field is very small and variations of 1 G are required. Fortunately, the "tiny hysteresis" demonstrates that after three cycles the behavior repeats itself.

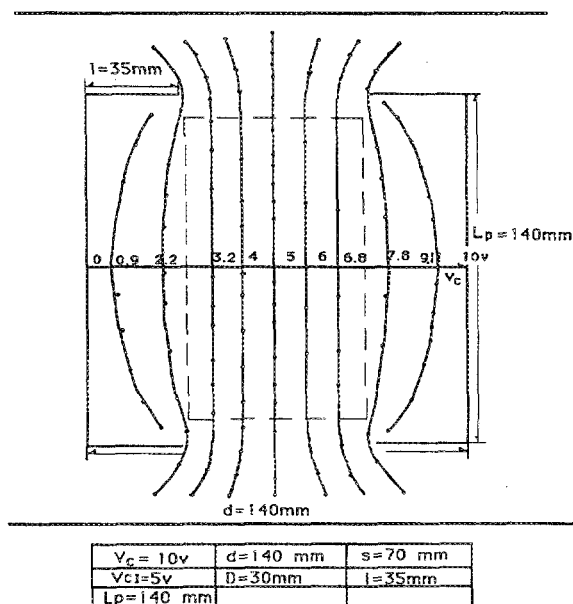


FIG. 9. Capacitor: The best configuration that produces a homogeneous electric field must have "wins" whose length is  $\frac{1}{4}$  of the separation distance between plates.

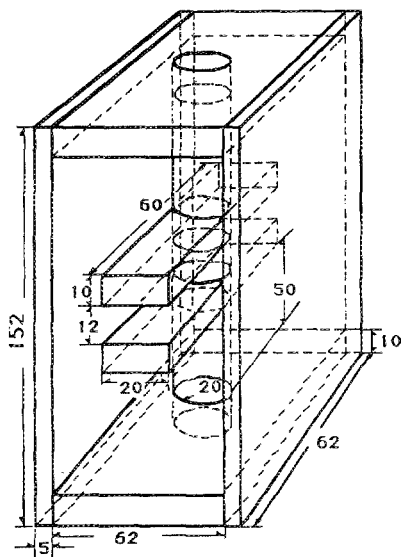


FIG. 10. Design of the magnet.

In order to test both types of Wien filters, an electron gun and a lithium-proton source<sup>11</sup> were built and their setup is shown in Figs. 13 and 14. A slit of 100  $\mu\text{m}$  diameter was used at the entrance and exit of the filter.

## V. RESULTS

As was expected, the spectrum and the envelope for electrons and protons in the analyzer with the classical parallel-rectangular magnetic poles show two peaks of high intensity, one at  $\phi_0 = \phi_d$ , which corresponds to  $z = \pi R_0$  or the energy focus, and the highest peak at  $\phi = 2\phi_d$ , which corresponds to  $z = 2\pi R_0$  or the mass focus. In order to plot  $I$  (detected current) vs  $E$  (electric field),  $E$  was varied and  $I$  was measured keeping  $E/B = \text{const}$ . The energy of the particles was chosen by setting the cathode voltage,  $\phi_0$ .

For the tilted-poles Wien filter, a single large peak was found in the spectrum of electrons and ions corresponding to

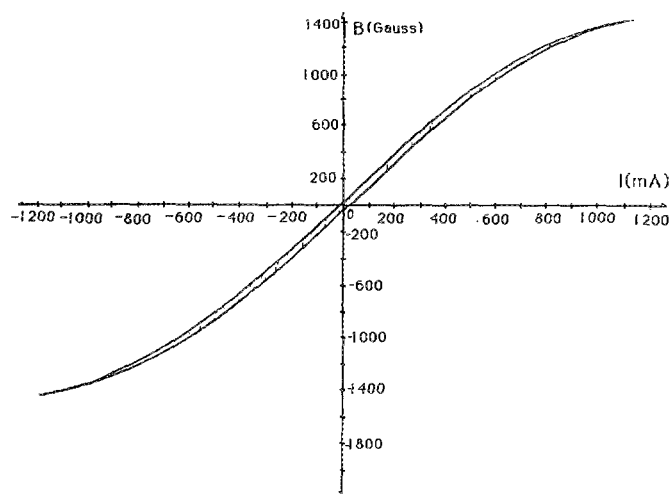


FIG. 11. Hysteresis of the magnet.

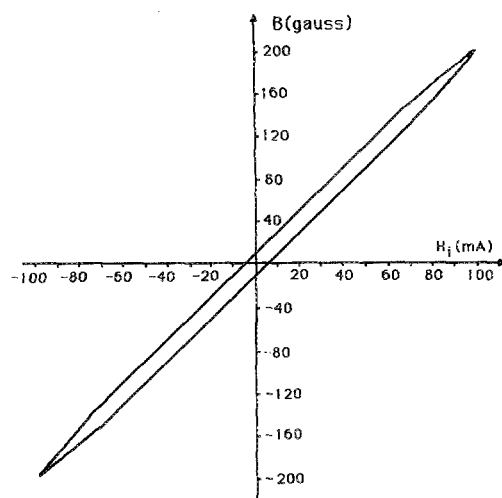


FIG. 12. "Tiny hysteresis."

the mass focus. This result agrees with that of Seliger<sup>10</sup> due to the elimination of astigmatism in the mass focus, but not in the energy focus. The spectrum for this case is shown in Figs. 15–18. In the plateau region, the particles have no deflection. The small peaks under the envelope indicate that the intensity corresponds to the trajectory of the beam. For this reason the narrowest peak under the envelope coincides with the mass focus.

In Figs. 19 and 20 a comparison of the behavior for electrons and protons between both Wien filters studied are shown, where clearly in the mass focus the intensity of the peak is higher for the tilted-poles Wien filter than for the parallel-rectangular-pole Wien filter for the same particle energy. (As shown previously, there is no energy focus in the tilted Wien filter.) The resolution of the analyzer is compared with that of a mass spectrometer of 90° in Fig. 21. We have also found that the tilted-poles Wien filter has outstanding resolution and sensitivity (higher than the classical design).

## VI. CONCLUSIONS

For the parallel-rectangular-poles Wien filter, an energy focus and a mass focus were found for electrons and protons, with a resolution of 2.2%. This result indicates that the two main functions of the Wien filter as an energy and mass ana-

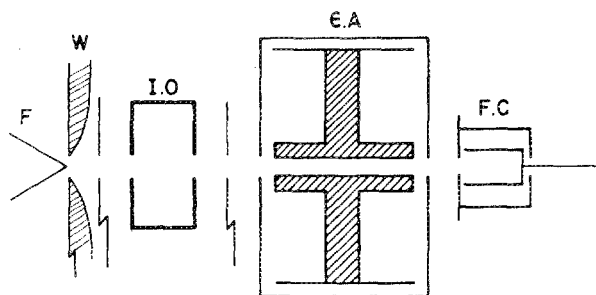


FIG. 13. Assembly of the system for electrons.

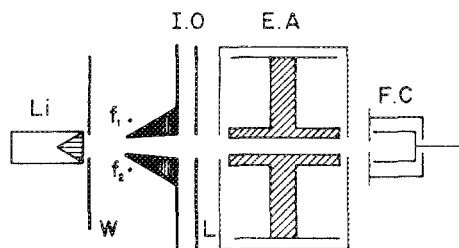


FIG. 14. Assembly of the system for protons.

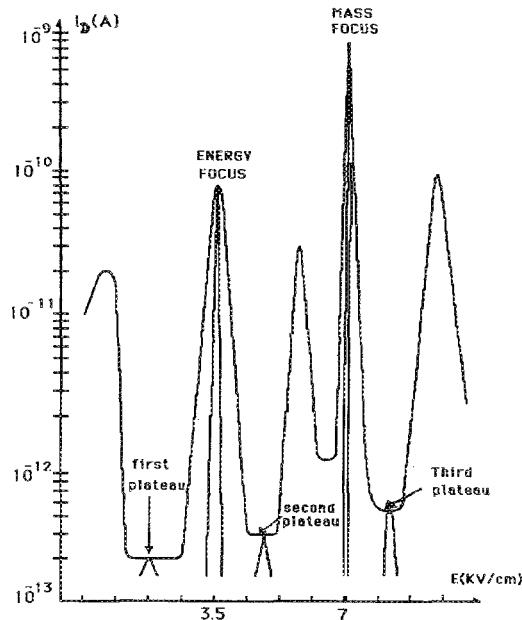


FIG. 15. Spectrum and envelope for electrons of 3500 eV in the parallel Wien filter. The electric field between the plates of the capacitor is 3500 V/cm for the energy focus and 7000 V/cm for the mass focus.

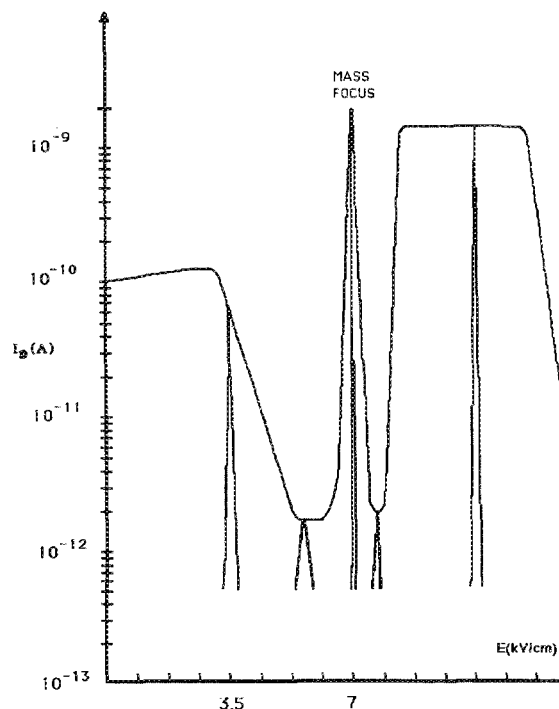


FIG. 16. Spectrum and envelope for electrons of 3500 eV in the tilted Wien filter. The electric field for the mass focus is 7000 V/cm between the plates of the capacitor.

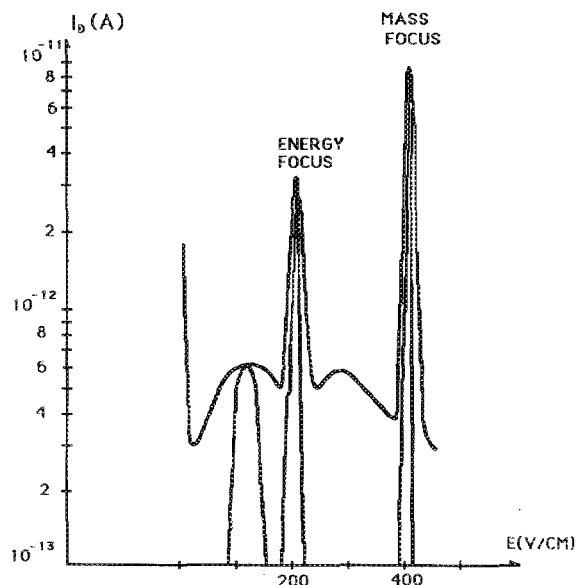


FIG. 17. Spectrum and envelope for protons of 200 eV in the parallel Wien filter. The electric field between the deflecting plates of the capacitor is 200 V/cm for the energy focus and 400 V/cm for the mass focus.

lyzer provide more information and better resolution than a mass spectrometer. The resolution of the tilted-poles Wien filter is about 30% better than the classical design.

It was also found that there is a high transparency and selectivity in both of the Wien filters studied, despite the small diameter of the entrance and exit apertures. For a 100- $\mu$ m-diam aperture, the maximum current observed in the mass focus was

$$I_{\max} = 10^5 \times I_0,$$

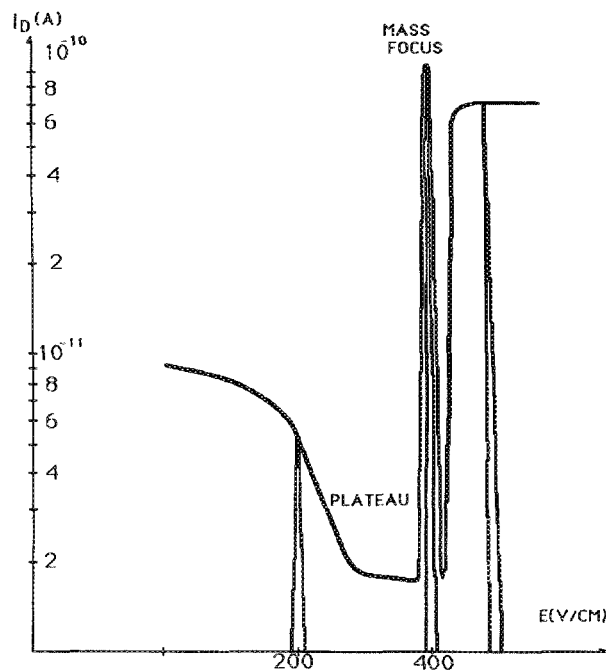


FIG. 18. Spectrum and envelope for protons of 200 eV in the Wien filter with tilted poles. The mass focus corresponds a deflecting electric field of 400 V/cm between the plates of the capacitor.

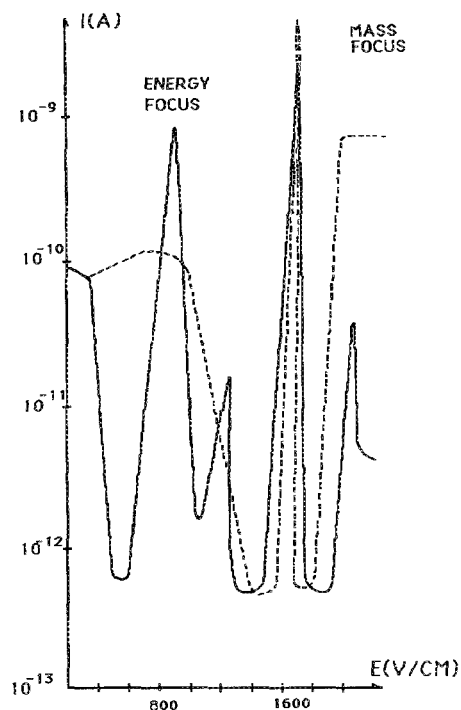


FIG. 19. Comparison of the spectrum of electrons of 800 eV for both Wien filters. Clearly, for the mass focus the peak in the tilted Wien filter is high as an indication of the elimination of the astigmatism: classic Wien filter (solid curve), tilted-poles Wien filter (dashed curve).

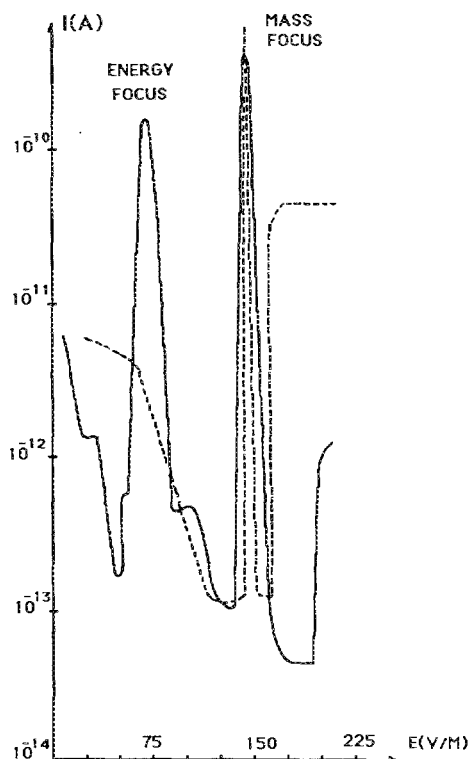


FIG. 20. Comparison of the spectrum for protons of 75 eV between the two filters. The dashed line corresponds to the spectrum of the tilted poles, where the astigmatism is eliminated in the mass focus.

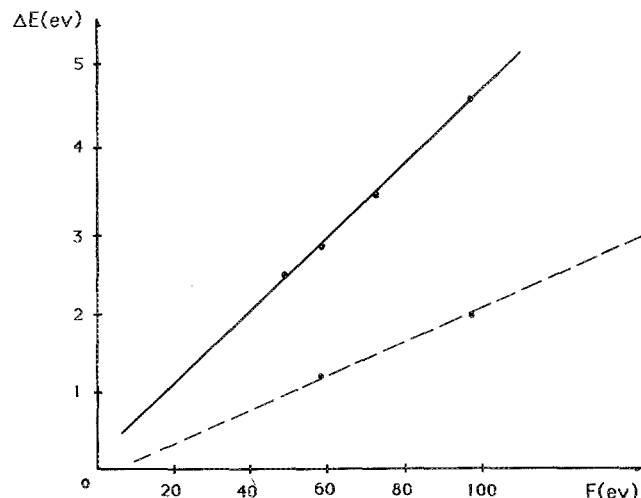


FIG. 21. Comparison of the resolution between the Wien filter and a mass spectrometer of 90°. Clearly, the resolution of the Wien filter is superior: mass spectrometer (solid curve), classic Wien filter (dashed curve).

where  $I_0$  is the collected current in the detector (Faraday cup) without fields and  $I_{\max}$  is the maximum current in the detector at the mass focus with fields.

A comparison between both analyzers can be made using the relation between  $I_{\max}$  and  $I_0$ ,

$$\frac{(I_{\max}/I_0)_{\text{Tilted}}}{(I_{\max}/I_0)_{\text{Rectangular}}} = 1.32.$$

The advantage belongs to the tilted-poles Wien filter. There is also clear indication from the experimental evidence that astigmatism is greatly reduced in the tilted-poles Wien filter.

The Wien filter is an indispensable diagnostic device for energetic charged particles (both electrons and ions). This diagnostic can analyze simultaneously the mass and energy of charged particles, with the additional advantage that the beam need not be curved as is the case with current diagnostic systems. Furthermore, the Wien filter has a much higher mass and energy resolution than do conventional mass and energy analyzers. We have developed a new type of Wien filter using a tilted-poles design and have shown this design to have higher resolution than the classical parallel-rectangular-poles design. We are presently exploring the potential of this new Wien filter as a high-temperature plasma diagnostic on the Missouri Magnetic Mirror (MMM) experiment.<sup>12</sup>

## ACKNOWLEDGMENTS

One of the authors (E. L.-Q.) is indebted to Martin Wilmers for very important suggestions for the development of this work and with all members of the Department of Physics at National University of Colombia, Bogota, for the support and discussion. We both would like to thank our colleagues in the Fusion Research Laboratory at the University of Missouri-Columbia for their help in wording and editing this paper. Finally, we would like to acknowledge the support of the National Science Foundation, Grant No. CBT-8352345, and the Department of Energy, Grant No. DE-FG02-87ER53255.A000.

- <sup>a)</sup> The abstract for this paper appears in the Proceedings of the 7th Topical Conference on High Temperature Plasma Diagnostics, Rev. Sci. Instrum. **59**, 1738 (1988).
- <sup>1</sup>K. W. Ogilvie, R. I. Kittridge, and T. D. Wilkerson, Rev. Sci. Instrum. **39**, 459 (1968).
- <sup>2</sup>H. Ewald and S. Garbes, Phys. Verh. **5**, 104 (1954).
- <sup>3</sup>J. Geiger (private communication).
- <sup>4</sup>G. H. Gurtis and J. Silcox, Rev. Sci. Instrum. **42**, 630 (1971).
- <sup>5</sup>K. Yano and Suck Hee Be, Jpn. J. Appl. Phys. **19**, 1019 (1980).
- <sup>6</sup>S. Galabella and D. P. Grubb, "Evaluation of Ion-Energy Spectrometers for use on MFTF," LLNL Report No. UCID19776, 12 April 1983.
- <sup>7</sup>S. D. Scott *et al.*, Nucl. Fusion **25**, 359 (1985).
- <sup>8</sup>E. Leal-Quiros, J. Appl. Phys. **52**, 1152 (1981).
- <sup>9</sup>M. Wilmers, "Instrumentation II," Lecture notes, National University of Colombia, Department of Physics, Bogota, Colombia, 1975.
- <sup>10</sup>R. L. Seliger, J. Appl. Phys. **43**, 2352 (1972).
- <sup>11</sup>P. Orozco and M. Wilmers, in Proceedings of the Ninth ICPEAC, Seattle, WA, 1975.
- <sup>12</sup>J. F. Kunze, M. A. Preias, T. J. Dolan, P. Bennet, J. Freeman, L. Haynes, J. Hwang, S. McGhee, and R. Roberts, Nucl. Technol. Fusion **10**, 1034 (1986).